Desalination and Water Treatment
www.deswater.com

36 (2011) 152–163
December

1944-3994/1944-3986
doi: 10.5004/dwt.2011.2250

Analysis of transmembrane electrical potential across nanofiltration membranes based on electrostatic and steric-hindrance model

Cong-Hui Tu, Yan-Yan Fang, Xiao-Lin Wang*

State Key Laboratory of Chemical Engineering, Department of Chemical Engineering, Tsinghua University, Beijing 100084, P.R.China
Tel./Fax: +861062794741(2); email: xl-wang@ tsinghua.edu.cn

Received 13 September 2010; accepted 7 March 2011

ABSTRACT

Transmembrane electrical potential (TMEP) across nanofiltration (NF) membranes was calculated analytically in single electrolyte solution — NF membranes systems with electrostatic steric-hindrance (ES) model in this study. Moreover, a simplified expression with average membrane parameters was obtained to give explicit explanations by combining ES model and irreversible thermodynamics. The effects of electrolyte species with common co-ion Cl^- (KCl and $MgCl_2$), electrolytes concentration c, diffusion coefficient ratio of co-ion over counterion D_2/D_1, pore radius r_p, ratio of membrane thickness over porosity $\Delta x/A_k$, effective volume charge density X_w on TMEP were investigated. The results showed that with the existence of membrane potential, dependencies of TMEP on solution flux were nonlinear. When ξ_f^{-1} ($z_1v_1c_f/X_w$) was larger than 50 for 1-1 electrolytes and 100 for 2-1 electrolytes, TMEP tended to be constant and three potentials (TMEP, membrane potential and convection potential) crossed at $D_2/D_1D_i = 1.0$, which implied that the electrostatic effect could be neglected. When the isoelectric point of membranes is judged in different pH based on the zero point of TMEP, solutes with $D_2/D_1 = 1.0$ is recommendatory. Because when $D_2/D_1 > 1.0$, the zero point will locate on where X_w is negative, and when $D_2/D_1 < 1.0$, zero points will appear when X_w is positive, and only when $D_2/D_1 = 1.0$, the zero point of TMEP appears when membrane is neutral (X_w is zero). Moreover, a sufficient condition $t_{1m}/z_1+t_{2m}/z_2 = 0$ was proposed to explain the coincidence of zero point of membrane potential and minimum of reflection coefficient.

Keywords: Transmembrane electrical potential; Nanofiltration membranes; The electrostatic and steric-hindrance model; Irreversible thermodynamics

1. Introduction

As an important electrokinetic phenomenon of nanofiltration (NF), transmembrane electrical potential (TMEP) was studied to promote understanding of transport mechanism of electrolytes in NF process [1–5]. TMEP is composed of three potentials (convection potential $\Delta\varphi_c$, diffusion potential $\Delta\varphi_d$ and donnan potential $\Delta\varphi_D$) accompanied by the coinstantaneous pressure drop and concentration difference between feed and permeate side. Convection potential is caused by the flux of electrolytes in the charged pores under the pressure gradient. Owing to the concentration difference in NF membranes, electrolytes will diffuse from high-concentration side to low-concentration side, and the different mobility between anion and

*Corresponding author

cation leads to the accumulation of high-mobility ions on the low-concentration side. As a result, diffusion potential is built up by the imbalance of anion and cation and concentration difference. Donnan potential is the electrical potential at the interfaces (feed-membrane and membrane-permeate), which is usually combined with diffusion potential as membrane potential to be discussed.

Compared with other method, such as, tangential streaming potential and membrane potential [6–9], TMEP has its own advantage. Tangential streaming potential can obtain the charge density of outer membranes surfaces, but possible differences in chemistry of inner and outer membrane surfaces can exist according to Lettmann [10]. The measurement of membrane potential is carried out under the condition with zero pressure drops without contribution of convection, and the concentration profiles in membranes are different from the ones during filtration process. On the contrary, TMEP can be measured simultaneously with the rejection in NF process under the same conditions. Therefore, it can actually reflect not only the relationship between the separation performance and electrokinetic phenomenon, but also the actual volume charge density of NF membranes in filtration process. The simultaneous measurement of TMEP and rejection in NF process makes it potential to actualize the on-line monitoring and diagnose for membrane fouling. Although its advantage, only a few studies were carried out to study TMEP [1–5,11,12]. Especially, the investigation of effect of outer solution and membrane characters on TMEP was not enough, extremely. Therefore, it is important and valuable to research TMEP for its convenience and sensitivity to change of outer solution, interface and membrane characters.

Many commercial NF membranes were proved to have pores with radii smaller than 1 nm, which were comparable to the inorganic ions. Not only the electrostatic effect but also the steric-hindrance effect should be taken into consideration. The ions flux and the mobility diversity between anion and cation, which were crucial factors on TMEP, would be influenced by the electrostatic effect due to the different valences and the steric-hindrance effect owing to the different radius of ions. In our preceding papers [13,14], the electrostatic and steric-hindrance model (ES model) was proposed and had already been verified in the permeation experiments of a mixture of a tracer organic electrolyte, and the results showed the steric-hindrance effect should not be ignored in NF membranes with small pores. Since ES model is successfully applied on prediction of separation performance in NF process, it should be an appropriate model of great promise to provide the information of TMEP theoretically. However, the research on TMEP by ES model has not been sufficient yet.

In this paper, ES model was employed to calculate TMEP. The expression of TMEP based on ES model was obtained for 1-1 electrolytes and 2-1 electrolytes. Moreover, in order to simplify the complicated expression of TMEP, an approximate equation was deduced based on the average membrane parameters by combining the ES model and irreversible thermodynamics. With the help of the accurate calculation by ES model and the approximate expression by average membrane parameters, the influence of solution characters (ion species, concentration, diffusion coefficient ratio of co-ion over counterion), membrane physical structure (ratio of membrane thickness over porosity, pore size) and electrical charge parameter (the effective volume charge density) on TMEP, convection potential and membrane potential were discussed adequately. This work raised the understanding of the transport mechanism of electrolytes across NF membranes and provided the crucial instruction for application of TMEP on on-line monitoring and diagnose.

2. Theory

The ES model assumes that membranes can be regarded as a bundle of capillaries with the pore radius r_p, the ratio of membrane thickness over membrane porosity $\Delta x/A_k$ and the effective membrane volume charge density X_w. The size of ions cannot be ignored when the pore radius and ion radius are on the equal order of magnitude. The activity coefficient that arises as a result of ion–ion interactions is taken to be unit. The ions are simulated as a rigid sphere of stokes radius r_s related to the diffusivity in dilute aqueous solution by the Stokes-Einstein equation. And the steric-hindrance effect of ions through the membrane capillaries can be demonstrated by the steric-hindrance pore model [15].

By taking into account both electrostatic interaction and steric-hindrance effects, the Nernst-Planck equation which describes the ion flux J_i can be expressed by the following modified equation [13]

$$J_i' = -D_{ip}\frac{dc_i(x)}{dx} - \frac{z_i F}{R_g T} D_{ip} c_i(x)\frac{d\varphi}{dx} + K_{ic} c_i(x) J_v'. \quad (1)$$

With $J_i' = J_i/A_k$, $J_v' = J_v/A_k$.

J_i', J_v', and J_i, J_v are the ion flux and volume flux over the capillary cross-section and the membrane surface, respectively. R_g, T and F are gas constant, temperature and Faraday constant. c_i is the concentration of ion i in membranes. D_{ip} is the effective ion diffusivity in membranes, equaling to $D_{ip} = D_i K_{id}$, D_i is diffusion

coefficient of ion i. K_{ic} is the convective hindrance factor. The expressions for K_{id} and K_{ic} are written as follows:

$$K_{id} = S_{Di}H_{Di}$$
$$K_{ic} = S_{Fi}H_{Fi}$$

Here, H_{Di} and H_{Fi} are called the steric-hindrance parameters related to the wall correction factors of ion i under diffusion and convection conditions, respectively, and expressed by the steric-hindrance pore model.

$$H_{Di} = 1$$
$$H_{Fi} = 1 + \frac{16}{9}\eta_i^2, \quad \eta_i = r_{si}/r_p$$

S_{Di} and S_{Fi} are the contribution to the averaged distribution coefficients caused by the steric-hindrance effects of ions under diffusion and convection conditions, and defined as follows:

$$S_{Di} = (1-\eta_i)^2$$
$$S_{Fi} = (1-\eta_i)^2[2-(1-\eta_i)^2]$$

The distribution coefficients can be calculated by the Donnan equilibrium or the Poisson-Boltzmann equation [13]. Here, the Donnan equilibrium is used for its simplification. Otherwise, the steric-hindrance effect is also taken into account. Nevertheless, the dielectric exclusion effect [16] and image force [17] are not included. Although these effects proved non-negligible on distribution of ions in membranes, they are too complex to be evaluated. In this paper, only the electrostatic effect and steric-hindrance effect are considered. The distribution coefficients in feed side and permeate side $k_i^{f(p)}$ are given.

$$k_i^{f(p)} = \frac{c_i}{c_i^{f(p)}} = S_{Di}\exp\left(-\frac{z_i F\Delta\varphi_D^{f(p)}}{R_g T}\right). \tag{2}$$

The superscript f and p mean the feed side and permeate side. So the Donnan potential can be calculated by the distribution coefficient

$$\Delta\varphi_D^{f(p)} = -\frac{R_g T}{z_2 F}\ln\left(\frac{k_2^{f(p)}}{S_{D2}}\right). \tag{3}$$

Electroneutrality in membranes and the external solution is expressed, respectively, as follows:

$$z_1c_1(x) + z_2c_2(x) + X_w = 0 \qquad \text{(inside membranes)} \tag{4a}$$

$$z_1c_1^{f(p)} + z_2c_2^{f(p)} = 0 \qquad \text{(external solution)} \tag{4b}$$

X_w is the effective volume charge density. Take Eq. (2) into electroneutrality condition, and therefore,

$$k_1^{f(p)} - k_2^{f(p)} + \xi_{f(p)} = 0. \tag{5}$$

With

$$\xi_{f(p)} = X_w/\left(z_1c_1^{f(p)}\right).$$

Introduce $\theta_{f(p)}$ into Eq. (5), $\theta_{f(p)}$ is expressed as follows:

$$\theta_{f(p)} = \exp\left(-\Delta\varphi_D^{f(p)}F\Big/R_gT\right).$$

Therefore $k_i = S_{Di}\theta_{f(p)}{}^{zi}$, and Eq. (5) can be rewritten as:

$$S_{D1}\theta_f^{z_1} - S_{D2}\theta_f^{z_2} + \xi_f = 0. \tag{6}$$

Concerning 1-1 electrolyte, $\theta_{f(p)}$ can be expressed easily by quadratic equation in one variable

$$\theta_{f(p)} = \frac{-\xi_{f(p)} + \sqrt{\xi_{f(p)}^2 + 4S_{D1}S_{D2}}}{2S_{D1}}. \tag{7}$$

For 2-1 electrolyte, $\theta_{f(p)}$ is relatively more complicated, and with the help of Cardano formula, the expressions are given [18],

$$\theta_{f(p)} = \begin{cases} \sqrt[3]{\frac{S_{D2}}{2S_{D1}} + \sqrt{\left(\frac{S_{D2}}{2S_{D1}}\right)^2 + \left(\frac{\xi_{f(p)}}{3S_{D1}}\right)^3}} \\ + \sqrt[3]{\frac{S_{D2}}{2S_{D1}} - \sqrt{\left(\frac{S_{D2}}{2S_{D1}}\right)^2 + \left(\frac{\xi_{f(p)}}{3S_{D1}}\right)^3}} \\ \left(\left(\frac{S_{D2}}{2S_{D1}}\right)^2 + \left(\frac{\xi_{f(p)}}{3S_{D1}}\right)^3 \geq 0\right) \\ 2\sqrt{-\frac{\xi_{f(p)}}{3S_{D1}}}\cos\frac{t_{f(p)}}{3}, t_{f(p)} = a\cos\frac{S_{D2}/S_{D1}}{2\sqrt{-\left(\frac{\xi_{f(p)}}{3S_{D1}}\right)^3}} \\ \left(\left(\frac{S_{D2}}{2S_{D1}}\right)^2 + \left(\frac{\xi_{f(p)}}{3S_{D1}}\right)^3 < 0, \frac{\xi_{f(p)}}{3S_{D1}} < 0\right) \end{cases} \tag{8}$$

In steady-state NF, the zero electrical current condition is given by,

$$F\sum_{i=1}^{2} z_i J_i' = 0 \tag{9}$$

And Eqs. (1) and (9) lead to the electrical potential gradient equation

$$\frac{\mathrm{d}\varphi}{\mathrm{d}x} = \frac{R_\mathrm{g}T}{F}\left(\frac{\sum_{i=1}^{2} -z_i D_{i\mathrm{p}} \frac{\mathrm{d}c_i}{\mathrm{d}x}}{\sum_{i=1}^{2} z_i^2 D_{i\mathrm{p}} c_i} + \frac{\sum_{i=1}^{2} J_v'(z_i K_{ic} c_i)}{\sum_{i=1}^{2} z_i^2 D_{i\mathrm{p}} c_i}\right). \tag{10}$$

The first term on right side is diffusion potential caused by ions diffusion, and the second term is convection potential. Diffusion potential depends on the concentration gradient, while convection potential is approximately linear to solution volume flux.

Integrating Eq. (10), TMEP is expressed [11]

$$\begin{aligned}\Delta\varphi_\mathrm{T} &= \Delta\varphi_\mathrm{D}^\mathrm{f} - \Delta\varphi_\mathrm{D}^\mathrm{p} + \Delta\varphi = \Delta\varphi_\mathrm{D}^\mathrm{f} - \Delta\varphi_\mathrm{D}^\mathrm{p} + \varphi(\Delta x^-) - \varphi(0^+) \\ &= \frac{R_g T}{F}\left\{\begin{array}{l} \dfrac{1}{z_2}\ln\dfrac{k_2^\mathrm{p}}{k_2^\mathrm{f}} + \dfrac{D_{1\mathrm{p}} - D_{2\mathrm{p}}}{z_2 D_{2\mathrm{p}} - z_1 D_{1\mathrm{p}}}\ln\dfrac{T_r k_2^\mathrm{p} - \tau_1\xi_\mathrm{f}}{k_2^\mathrm{f} - \tau_1\xi_\mathrm{f}} \\ +A\ln\dfrac{T_r k_2^\mathrm{p} - \tau_1\xi_\mathrm{f}}{k_2^\mathrm{f} - \tau_1\xi_\mathrm{f}} + \dfrac{B}{2}\ln\dfrac{f(T_r k_2^\mathrm{p})}{f(k_2^\mathrm{f})} \\ +\dfrac{2C - B\alpha(T_\mathrm{r})}{2\sqrt{p(T_\mathrm{r})}}\ln\left[\dfrac{\left(\sqrt{p(T_\mathrm{r})} + f'(k_2^\mathrm{f})\right)\left(\sqrt{p(T_\mathrm{r})} - f'(T_r k_2^\mathrm{p})\right)}{\left(\sqrt{p(T_\mathrm{r})} - f'(k_2^\mathrm{f})\right)\left(\sqrt{p(T_\mathrm{r})} + f'(T_r k_2^\mathrm{p})\right)}\right] \end{array}\right\}\end{aligned} \tag{11}$$

With

$$A = \frac{D_\mathrm{s}}{w(z_2 D_{2p} - z_1 D_{1\mathrm{p}})}\left[\left(1 - \frac{D_{1\mathrm{p}}}{D_{2\mathrm{p}}}\right)\frac{1}{1-v}\left(K_{2\mathrm{c}} - K_{1\mathrm{c}} + \frac{K_{1\mathrm{c}}}{\tau_1}\right)\right]$$

$$B = \frac{D_\mathrm{s}}{w(z_2 D_{2\mathrm{p}} - z_1 D_{1\mathrm{p}})}\left[(K_{2\mathrm{c}} - K_{1\mathrm{c}}) - \left(1 - \frac{D_{1\mathrm{p}}}{D_{2\mathrm{p}}}\right)\frac{1}{1-v}\left(K_{2\mathrm{c}} - K_{1\mathrm{c}} + \frac{K_{1\mathrm{c}}}{\tau_1}\right)\right]$$

$$C = \frac{D_\mathrm{s}}{w(z_2 D_{2\mathrm{p}} - z_1 D_{1\mathrm{p}})}\left\{\frac{K_{1\mathrm{c}}}{\tau_1(1-v)}\left[\frac{T_\mathrm{r}}{w}\left(1 - \frac{D_{1\mathrm{p}}}{D_{2\mathrm{p}}}\right) - \varepsilon\right] + \frac{T_\mathrm{r}}{w}\frac{K_{2\mathrm{c}} - K_{1\mathrm{c}}}{1-v}\left(1 - \frac{D_{1\mathrm{p}}}{D_{2\mathrm{p}}}\right)\right\}$$

$$D_\mathrm{s} = \frac{D_{1\mathrm{p}} D_{2\mathrm{p}}(z_1 - z_2)}{z_1 D_{1\mathrm{p}} - z_2 D_{2\mathrm{p}}}$$

$$w = K_{2\mathrm{c}}\tau_1 - K_{1\mathrm{c}}\tau_2, \qquad \tau_i = \frac{z_i D_{i\mathrm{p}}}{z_1 D_{1\mathrm{p}} - z_2 D_{2\mathrm{p}}}, \qquad i = 1, 2$$

$$v = -v_1/v_2, \quad \lambda = -\frac{\xi_\mathrm{f}}{1-v}$$

$$\alpha(T_\mathrm{r}) = -\xi_\mathrm{f} - T_\mathrm{r}/w, \qquad \beta(T_\mathrm{r}) = T_\mathrm{r}\xi_\mathrm{f}\tau_1/w$$

$$p(T_\mathrm{r}) = [\alpha(T_\mathrm{r})]^2 - 4\beta(T_\mathrm{r}) = \varepsilon^2 + \left(\frac{T_\mathrm{r}}{w}\right)^2 + 2\frac{T_\mathrm{r}\xi_\mathrm{f}\tau_1}{w}(1 - 2\tau_1)$$

$$f(x) = x^2 + \alpha(T_\mathrm{r})x + \beta(T_\mathrm{r})$$
$$f'(x) = 2x + \alpha(T_\mathrm{r})$$

T_r is the transmission, equaling to $1-R$. And diffusion potential and convection potential are:

$$\Delta\varphi_\mathrm{d} = \frac{R_\mathrm{g}T}{F}\left(\frac{D_{1\mathrm{p}} - D_{2\mathrm{p}}}{z_2 D_{2\mathrm{p}} - z_1 D_{1\mathrm{p}}}\ln\frac{T_\mathrm{r}k_2^\mathrm{p} - \tau_1\xi_\mathrm{f}}{k_2^\mathrm{f} - \tau_1\xi_\mathrm{f}}\right), \tag{12}$$

$$\Delta\varphi_\mathrm{c} = \frac{R_\mathrm{g}T}{F}\left\{\begin{array}{l} A\ln\dfrac{T_r k_2^\mathrm{p} - \tau_1\xi_\mathrm{f}}{k_2^\mathrm{f} - \tau_1\xi_\mathrm{f}} + \dfrac{B}{2}\ln\dfrac{f(T_r k_2^\mathrm{p})}{f(k_2^\mathrm{f})} \\ +\dfrac{2C - B\alpha(T_\mathrm{r})}{2\sqrt{p(T_\mathrm{r})}}\ln\left[\dfrac{\left(\sqrt{p(T_\mathrm{r})} + f'(k_2^\mathrm{f})\right)\left(\sqrt{p(T_\mathrm{r})} - f'(T_r k_2^\mathrm{p})\right)}{\left(\sqrt{p(T_\mathrm{r})} - f'(k_2^\mathrm{f})\right)\left(\sqrt{p(T_\mathrm{r})} + f'(T_r k_2^\mathrm{p})\right)}\right] \end{array}\right\} \tag{13}$$

Combining diffusion potential, convection potential and Donnan potential, TMEP can be finally obtained. And also membrane potential can be expressed by summing up Donnan potential and diffusion potential.

$$\begin{aligned}\Delta\varphi_\mathrm{m} &= \Delta\varphi_\mathrm{D}^\mathrm{f} - \Delta\varphi_\mathrm{D}^\mathrm{p} + \Delta\varphi_\mathrm{d} \\ \Delta\varphi_\mathrm{T} &= \Delta\varphi_\mathrm{D}^\mathrm{f} - \Delta\varphi_\mathrm{D}^\mathrm{p} + \Delta\varphi = \Delta\varphi_\mathrm{m} + \Delta\varphi_\mathrm{c}\end{aligned} \tag{14}$$

It's difficult to analysis the rules of potentials from Eqs. (12) and (13), therefore the membrane parameters from irreversible thermodynamics are introduced to obtain a simpler expression.

From Eq. (1), the solute flux through capillaries $J_1' + J_2'$ and the electric current I are expressed as follows.

$$J_1' + J_2' = -\sum_{i=1}^{2} D_{i\mathrm{p}}\frac{\mathrm{d}c_i(x)}{\mathrm{d}x} - \frac{\sum_{i=1}^{2} z_i c_i(x) D_{i\mathrm{p}}}{R_\mathrm{g}T/F}\frac{\mathrm{d}\varphi}{\mathrm{d}x} + J_v'\sum_{i=1}^{2} K_{ic}c_i(x) \tag{15}$$

$$\begin{aligned}I = F\sum_{i=1}^{2} z_i J_i' = -F\Bigg[&\sum_{i=1}^{2} z_i D_{ip}\frac{\mathrm{d}c_i(x)}{\mathrm{d}x} - \frac{\sum_{i=1}^{2} z_i^2 c_i(x) D_{i\mathrm{p}}}{R_\mathrm{g}T/F}\frac{\mathrm{d}\varphi}{\mathrm{d}x} \\ &+ J_v'\sum_{i=1}^{2} z_i K_{ic}c_i(x)\Bigg]\end{aligned} \tag{16}$$

Combining Eq. (15) and Eq. (16), the solute flux $J_1' + J_2'$ can be rewritten:

$$J_1' + J_2' = \left\{ \begin{array}{l} \left[\sum_{i=1}^{2} c_i(x) K_{ic} - \frac{\left(\sum_{i=1}^{2} z_i c_i(x) K_{ic} \right) \times \left(\sum_{i=1}^{2} z_i c_i(x) D_{ip} \right)}{\left(\sum_{i=1}^{2} z_i^2 c_i(x) D_{ip} \right)} \right] J_v \\ + \left[- \sum_{i=1}^{2} D_{ip} \frac{dc_i(x)}{dx} + \frac{\left(\sum_{i=1}^{2} z_i c_i(x) D_{ip} \right)}{\sum_{i=1}^{2} z_i^2 c_i(x) D_{ip}} \sum_{i=1}^{2} z_i D_{ip} \frac{dc_i(x)}{dx} \right] \\ + \frac{\sum_{i=1}^{2} z_i c_i(x) D_{ip}}{\sum_{i=1}^{2} z_i^2 c_i(x) D_{ip}} \cdot \frac{I}{F} \end{array} \right\} \quad (17)$$

And the solute flux and the electric current also can be expressed by the irreversible thermodynamics, the following equations were proposed by Smit and co-workers [19]:

$$J_1' + J_2' = (\mathbf{1} - \sigma)(v_1 + v_2) c J_v - \omega R_g T (v_1 + v_2) c \frac{d \ln c}{dx} + \sum_{i=1}^{2} \frac{t_i}{z_i F} I \quad (18)$$

$$I = \frac{\kappa \beta}{L_p} J_V + \kappa \left(\frac{t_1}{z_1 F} + \frac{t_2}{z_2 F} \right) \left(-R_g T \frac{d \ln c}{dx} \right) + \kappa \left(- \frac{d\varphi}{dx} \right) \quad (19)$$

Comparing Eq. (17) with Eq. (18), and Eq. (19) with Eq. (16), the membrane parameters including electric transport number t_i, reflection coefficient σ, solute permeability coefficient ω, and electric conductance κ are written as follows.

$$t_i = \frac{z_i^2 D_{ip} c_i(x)}{\sum_{i=1}^{2} z_i^2 D_{ip} c_i(x)}, \quad i = 1, 2, \quad (20)$$

$$1 - \sigma = K_{1c} k_1 t_2 + K_{2c} k_2 t_1, \quad (21)$$

$$\omega = \frac{v_1 + v_2}{v_2} \frac{D_{2p} k_2 t_1}{R_g T}, \quad (22)$$

$$\kappa = \frac{F^2 \sum_{i=1}^{2} z_i^2 c_i(x) D_{ip}}{R_g T}. \quad (23)$$

Electric transport number t_i reflects the mobility of ion i in membranes, and reflection coefficient σ means the maximum rejection. Taking the expressions of t_i and κ into eq. 10, it can be rewritten:

$$\frac{d\varphi}{dx} = \sum_{i=1}^{2} \frac{t_i}{z_i F} \left(-R_g T \frac{d \ln c_i}{dx} \right) + \frac{i_c}{\kappa}. \quad (24)$$

With

$$i_c = \sum_{i=1}^{2} z_i K_{ic} c_i F J_v' \quad (25)$$

i_c is the convection current density. If transport numbers are considered as average transport numbers, and are treated as constancies in membranes, the potentials can be obtained by integrating Eq. (24) from feed side to permeate side as follows:

$$\Delta\varphi_T = \Delta\varphi_D^f - \Delta\varphi_D^p + \Delta\varphi = \Delta\varphi_m + \Delta\varphi_c = \sum_{i=1}^{2} \frac{t_{im} R_g T}{z_i F} \ln(1 - R) + \frac{i_{cm}}{\kappa_m / \Delta x} \quad (26)$$

where t_{im}, i_{cm} and κ_m are the average values of transport number, convection current density and electric conductance in membranes. The first term of right side in Eq. (26) is membrane potential, and the second one is convection potential. Eq. (26) is an approximate equation of Eq. (11), for t_i, i_c and κ change in x-direction in membranes factually. When proper average membrane parameters are chosen, there will be little difference between Eq. (11) and Eq. (26). In this paper, we will not concern about the choice of these average membrane parameters. Eq. (26) is used to obtain better understand the rules of potentials. Therefore, in Section 3, the figures are calculated by Eq. (11) and the explanations are mainly based on Eq. (26).

3. Results and discussion

According to the characters of some commercial NF membranes, the pore radius, ratio of membrane thickness over membrane porosity and effective volume charge density are chosen as 0.4 nm, 10^{-4} m and -100 mol .m^{-3} when the solution characters are consider as variables. And the solution volume flux ranges from 0 to 12 × 10^{-6} m^3 .m^{-2} s^{-1}; the concentration of electrolyte varies from 5mol.m^{-3} to 10,000 mol .m^{-3}; KCl and $MgCl_2$ are investigated except when diffusion coefficients ratio of co-ion over counterion is varied from 0.2 to 3.2. When investigation of membrane characters is carried out, radius ratio of co-ion over membrane pore, ratio of membrane thickness over membrane porosity and effective volume charge density range from r_{s1}/r_p = 0.01 to 0.76, from $\Delta x/A_k$

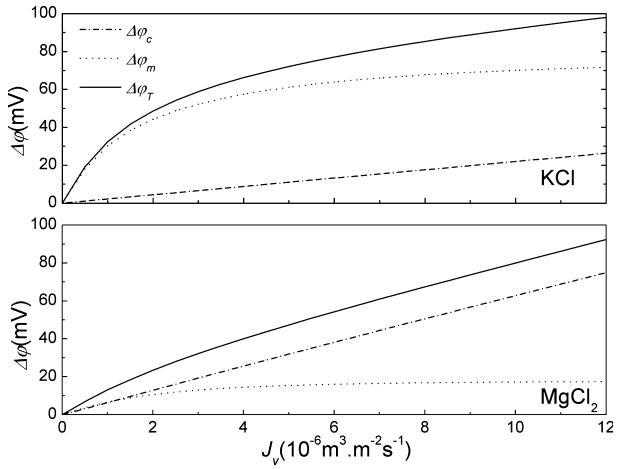

Fig. 1. Potentials as function of solution volume flux J_v (KCl and $MgCl_2$).c_f=10 mol m^{-3}; r_p = 0.4 nm; $\Delta x/A_k = 10^{-4}$m; $X_w = -100$ mol m^{-3}.

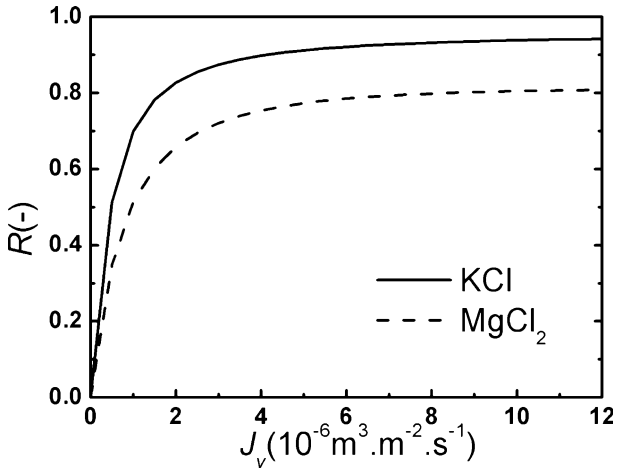

Fig. 2. Rejection as function of solution volume flux J_v (KCl and $MgCl_2$).$c_f = 10$ mol m^{-3}; $r_p = 0.4$ nm; $\Delta x/A_k = 10^{-4}$ m; $X_w = -100$ mol m^{-3}.

$=0.1 \times 10^{-4}$ to 5×10^{-4}m, and $X_w = -200$ to 200 mol .m^{-3}. The temperature is fixed at 20°C.

3.1. Effect of solution volume flux on potentials

In Fig.1, the relationship between potentials and solution volume flux J_v in KCl and $MgCl_2$ solution across NF membranes was exhibited. When solution volume flux increases, three potentials increase. Convection potential is approximately linear to solution volume, which can be deduced from Section 2, while membrane potential shows sub-linear. With the existence of membrane potential, the dependences of TMEP on the solution flux are nonlinear. Increase of solution volume flux leads to the increase of rejection in Fig. 2, which caused the increase of membrane potential. While solution volume flux is large enough, rejection will tend to a steady value, resulting in a flat curve of membrane potential. It can be forecasted that as flux is large enough, convection potential will be the dominant factor. In other words, TMEP will be approximately linear to solution volume flux, and this slope can be a substitute of the one of convection potential, which is usually called streaming potential.

TMEP and membrane potential of KCl are larger than $MgCl_2$, while convection potential is opposite. The phenomena can be explained by two reasons. First, as can be seen from Fig. 2, in the condition considered, rejection of $MgCl_2$ is smaller than KCl, therefore, membrane potential will be smaller for $MgCl_2$. Second, K^+ is more mobile than Mg^{2+} in membranes, which increases the transport number of K^+ and conductance of KCl in membranes, and they result in the increase of membrane potential and decrease of convection potential for KCl.

3.2. Effect of solution concentration on potentials

Fig. 3 shows the potential curves as a function of ξ_f^{-1} for KCl and $MgCl_2$ solution under constant pore radius of 0.4 nm, ratio of effective membrane thickness over membrane porosity of 1×10^{-4} m, effective volume charge density of −100 mol .m^{-3} and solution volume flux of 12×10^{-6} m^3 .m^{-2} s^{-1}. ξ_f^{-1} is proportional to feed concentration c_f, therefore, it is indicated that in Fig. 3 potentials decrease as feed concentration increase. In low concentration range, TMEP and membrane potential decrease sharply with the growth of feed concentration in KCl solution, which does no't occur in $MgCl_2$ solution. Convection potential tends to be constant when feed concentration is small enough in both KCl and $MgCl_2$ solution.

From Eq. (20), transport number mainly depends on the concentration and the diffusion coefficient difference of co-ion and counter-ion in membranes. For KCl solution, in low concentration range, with the increase of concentration, the rejection of KCl decreases sharply, meaning the sharp increase of concentration of Cl^-. Therefore, the transport number of Cl^- increases, while that of K^+ decreases. The difference of transport number of K^+ and Cl^- will become smaller. Membrane potential of KCl will decrease sharply due to the decrease of rejection and the difference of transport number of K^+ and Cl^-. In $MgCl_2$ solution, concentration of Mg^{2+} in membranes is low for its large size in this concentration range, and it restricts concentration of Cl^-, so the rejection shows little changes in Fig. 3b. Therefore, curve of membrane potential in $MgCl_2$ solution is flatter. Concentration of counterions is the dominate factor of convection potential in low concentration range. Under this condition, co-ion is

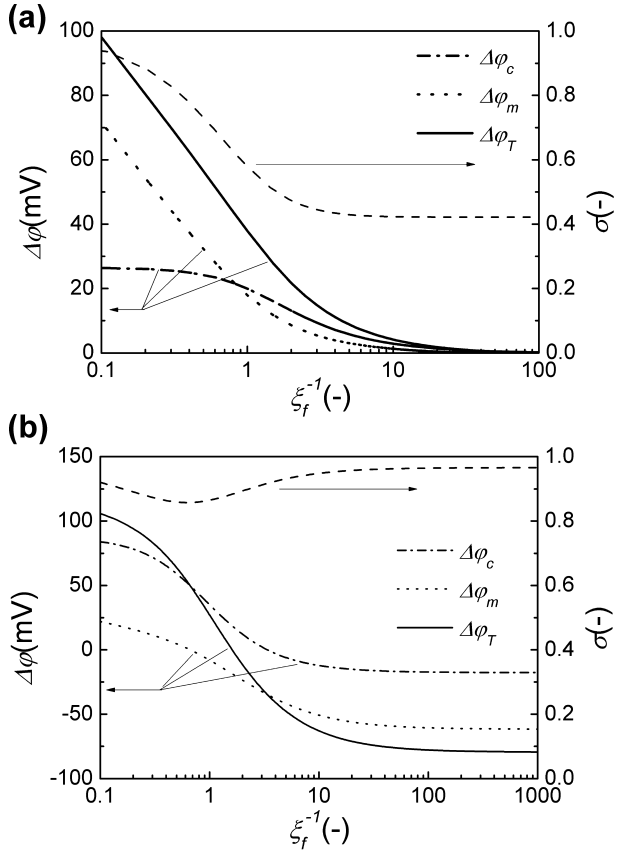

Fig. 3. Potentials and reflection coefficient as function of feed concentration ξ_f^{-1}. (a) KCl; (b) $MgCl_2$; $J_v = 12 \times 10^{-6}$ m^3 m^{-2} s^{-1}; $r_p = 0.4$ nm; $\Delta x/A_k = 10^{-4}$ m; $X_w = -100$ mol m^{-3}.

almost excluded outside membranes, and concentration of co-ion can be ignored, so concentration of counterions approximately equals to the volume charge density. Conductance and convection current will be constants if the volume charge density is fixed.

When ξ_f^{-1} is larger than 50 for KCl, and ξ_f^{-1} is larger than 100 for $MgCl_2$, potentials tend to be constant. Under these conditions, concentration of co-ions is comparable with counterions in membranes. It can be deduced that the electrostatic effect can be ignored and only hindrance-steric effect is considered. Then rejection and transport numbers of ions do nothing with the concentration, which just depend on the ratio of ions radius over pore radius. Therefore, curves of membrane potential are smooth in high concentration range. Convection potential is also constant in high concentration range for the counteraction of conductance and convection current, both of which are proportional to concentration. Without respect of the hindrance-steric effect, potentials, especially membrane potential of the electrolytes with $D_2/D_1 \neq 1$, such as $MgCl_2$, will tend to be zero with growth of feed concentration, which is different from the prediction by ES model.

It is worth to mention that when feed concentration is high enough, membrane potential of $MgCl_2$ will become negative, which does not happen in KCl. In bulk, transport number of Mg^{2+} is smaller than Cl^-, while in membranes, especially in low concentration range, the excess concentration of Mg^{2+} makes it possible that transport number of Mg^{2+} is larger than Cl^-, and under this situation, the sign of membrane potential is opposite to that in bulk. When feed concentration increases, the mobility of Mg^{2+} will be slowly weakened till equaling to the bulk, and when transport number of Mg^{2+} is lower than Cl^-, the sign of membrane potential changes. Because of the equivalent mobility of K^+ and Cl^- in bulk, K^+ in membranes always transports faster than Cl^-, and the sign of membrane potential will not change.

In Fig. 3, we found that reflection coefficient of KCl decreased with the growth of feed concentration, while the one of $MgCl_2$ decreased till a minimum value and then increased. It is more interesting that feed concentration when reflection coefficient of $MgCl_2$ obtains the minimum is the same as the one when membrane potential equals zero. This phenomenon was confirmed by the analysis in theory and the experimental results [20].

Moreover, when ξ_f^{-1} is larger than 50 for KCl, and for $MgCl_2$ when ξ_f^{-1} is larger than 100, the values of reflection coefficients of electrolytes will just depend on the hindrance-steric effect, and will not equal to zero, which is different from the results without consideration of hindrance-steric effect in some models (Fixed Charge Model or Space Charge Model) [21].

3.3. Effect of diffusion coefficients ratio of co-ion over counterion on potentials

Figs. 4 and 5 shows the potentials and rejection versus D_2/D_1 for 1-1 and 2-1 electrolytes with feed concentration of 10mol.m^{-3}, 500mol.m^{-3} and 5,000 mol .m^{-3}. In calculation process, the co-ion is taken as chlorine ion, and the counter-ion is fictitious ion and taken as variables. With the growth of D_2/D_1, in different concentration ranges, potentials present different behavior. In low concentration range, potentials monotonously increase as D_2/D_1 increases, and the influence of D_2/D_1 on convection potential is stronger than that on membrane potential. In middle concentration range, membrane and TMEP will decrease first and then increase. While in high concentration range, potentials will decrease as the growth of D_2/D_1. When ξ_f^{-1} is larger than 50 for 1-1 electrolytes, and for 2-1 electrolytes when ξ_f^{-1} is larger than 100, TMEP,

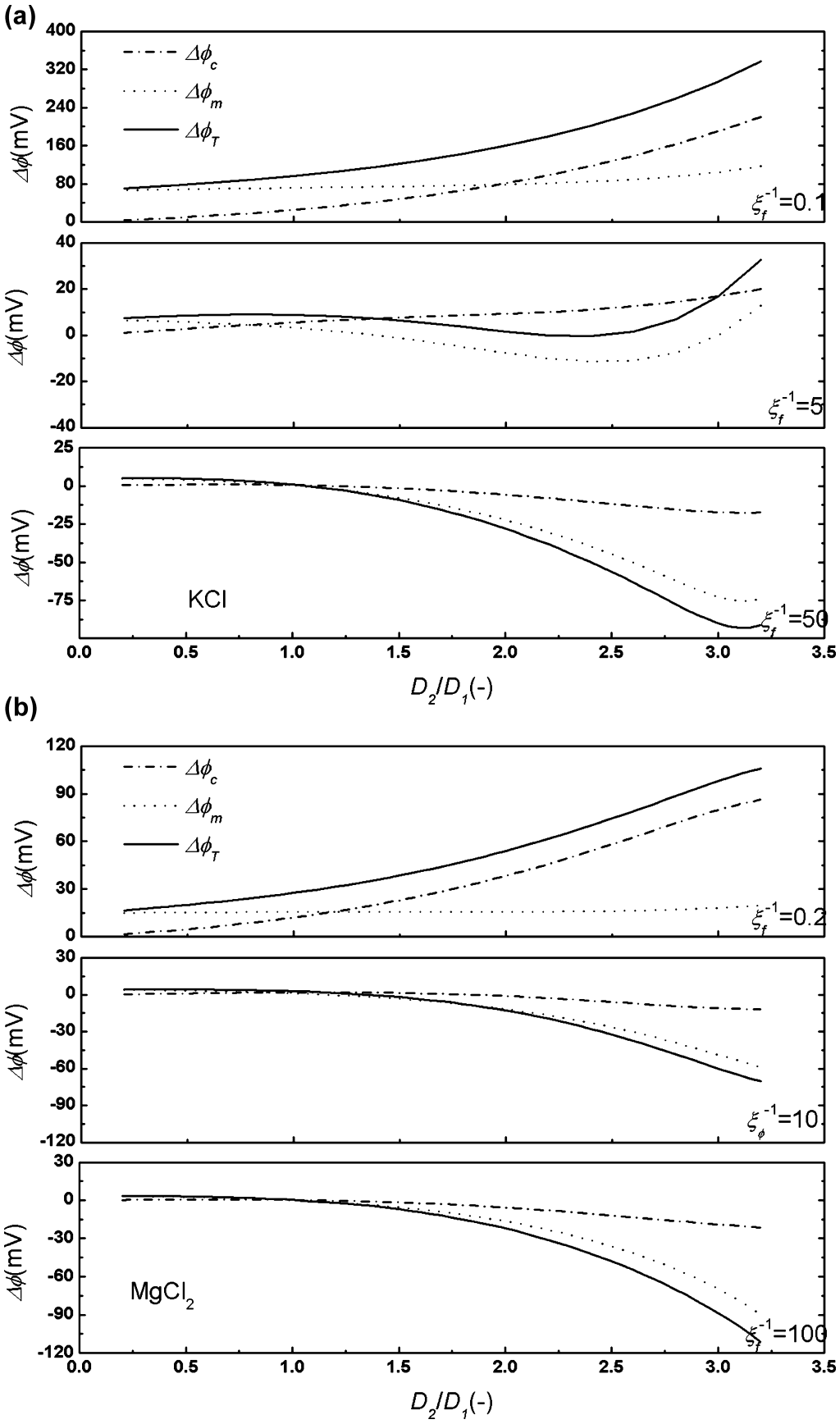

Fig. 4. Potentials as function of diffusion coefficients ratio of co-ion over counterion D_2/D_1. (a) 1-1 electrolyte; (b) 2-1 electrolyte; $J_v = 12 \times 10^{-6}$ m^3 m^{-2} s^{-1}; $r_p = 0.4$ nm; $\Delta x/A_k = 10^{-4}$ m;$X_w = -100$ mol m^{-3}.

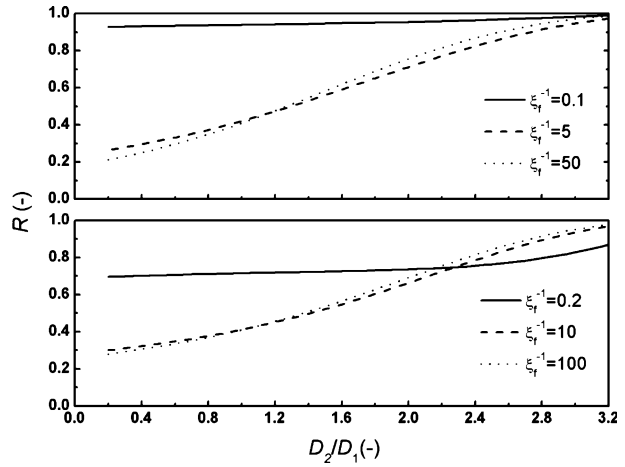

Fig. 5. Rejection as function of diffusion coefficients ratio of co-ion over counterion D_2/D_1. $J_v = 12 \times 10^{-6}$ m^3 m^{-2} s^{-1}; $r_p = 0.4$ nm; $\Delta x/A_k = 10^{-4}$ m; $X_w = -100$ mol m^{-3}.

membrane potential and convection potential will cross at one point, which is D_2/D_1=1.0.

The coinstantaneous change of diffusion coefficient and stokes radius gives arise to these phenomena. Furthermore, the different influence of electrostatic effect and hindrance-steric effect in different concentration range also bring on the different behaviors of potentials. The increase of D_2/D_1 means slower diffusion and larger size of counterions. In low concentration range, co-ions are almost repelled from membranes, and the transport number of co-ion is almost 1.0, so characters of counterions are the crucial factors. With the growth of D_2/D_1, the size of counterions increases, which causes the increase of rejection in Fig. 5 and membrane potential for the strong steric-hindrance effect. Increase of rejection means the decrease of concentration of counterions in membranes, resulting in the decrease of conductance. Therefore, convection potential increases as D_2/D_1 increases according to Eeq. (26). Without consideration of steric-hindrance effect the curves of potentials will be opposite to these obtained by ES model for the decrease of rejection with the increase of D_2/D_1. When concentration increases, the influence of co-ions should not be ignored. The slower diffusion of counterion can shorten difference of transport numbers between co-ions and counterions, causing the decrease of membrane potential. However, the increase of stokes radius of counterions still leads to the increase of membrane potential. Therefore, competition between decrease of difference of diffusion coefficient and increase of stokes radius of counterions brings on the curves of membrane potential. When feed concentration is large enough, the charges of membranes are screened, and concentration of co-ions is comparable to counterions.

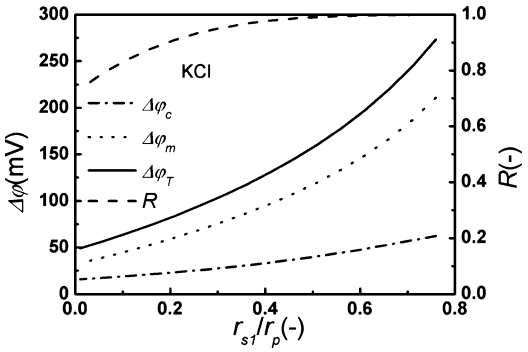

Fig. 6. Potentials and rejection as function of radius ratio of counterion over membrane pore r_{s1}/r_p in KCl solution. $c_f = 10$ mol m^{-3}; $J_v = 12 \times 10^{-6}$ m^3 m^{-2} s^{-1}; $\Delta x/A_k = 10^{-4}$ m; $X_w = -100$ mol m^{-3}.

The behaviors of potentials in membranes are just like in bulk. The potentials will cross at the point of $D_2/D_1 = 1$. If $D_2/D_1 < 1$, which directly means the mobility of co-ions is smaller than counterions, potentials are all positive. And If $D_2/D_1 > 1$, potentials are all negative.

3.4. Effect of pore radius and the ratio of membrane thickness over membrane porosity on potentials

Fig. 6 presents potentials and rejection as a function of radius ratio of counterion over membrane pore in KCl solution. As can be seen, the decrease of pore radius enlarges the potentials. When pore radius decreases, the steric-hindrance effect increases, so rejection increases and the solution concentration in membranes decreases. In other words, conductance in membranes decreases, resulting in increase of potentials as decrease of pore radius. If the steric-hindrance effect is neglected in membranes with small pores, the potentials will be underestimated.

As can be seen in Fig. 7, $\Delta x/A_k$plays obviously different roles on three potentials in KCl solution. Convection potential is almost linear to $\Delta x/A_k$, for $\Delta x/A_k$ is linear to hydrodynamic resistance in membranes. When $\Delta x/A_k$ is large enough, membrane potential tends to be steady. $\Delta x/A_k$ has nothing to do with reflection coefficient, but it determines how fast rejection reaches reflection coefficient. The longer $\Delta x/A_k$ is, the lower J_v is at which rejection levers off. For KCl, when $\Delta x/A_k$ is larger than 10^{-4} m, rejection nearly equals to the value of reflection coefficient. Slope of TMEP to $\Delta x/A_k$ is equal to that of convection potential at large $\Delta x/A_k$, which means at special J_v, increase of convection potential contributes almost 100% due to $\Delta x/A_k$.

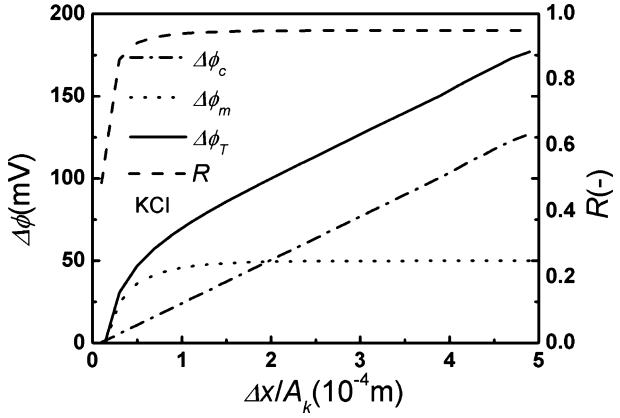

Fig. 7. Potentials and rejection as function of the ratio of membrane thickness over membrane porosity $\Delta x/A_k$ in KCl solution; $c_f = 10$ mol .m^{-3}; $J_v = 12 \times 10^{-6}$ m^3 m^{-2} s^{-1}; $r_p = 0.4$ nm; $X_w = -100$ mol m^{-3}.

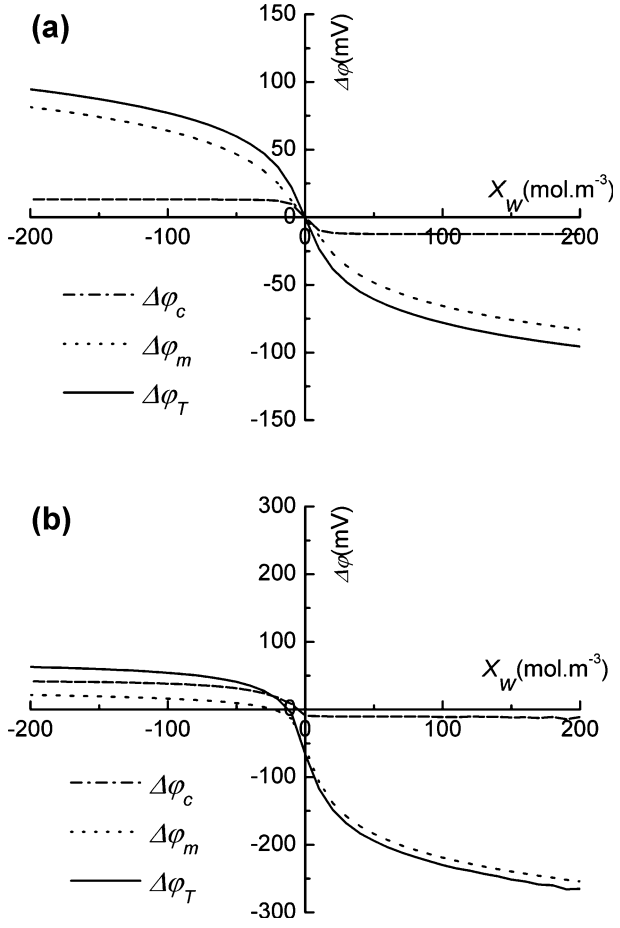

Fig. 8. Potentials as function of effective volume charge density X_w. (a) KCl; (b)$MgCl_2$; $c_f = 10$ mol m^{-3}; $J_v = 12 \times 10^{-6}$ m^3 m^{-2} s^{-1}; $\Delta x/A_k = 10^{-4v}$m; $r_p = 0.4$ nm.

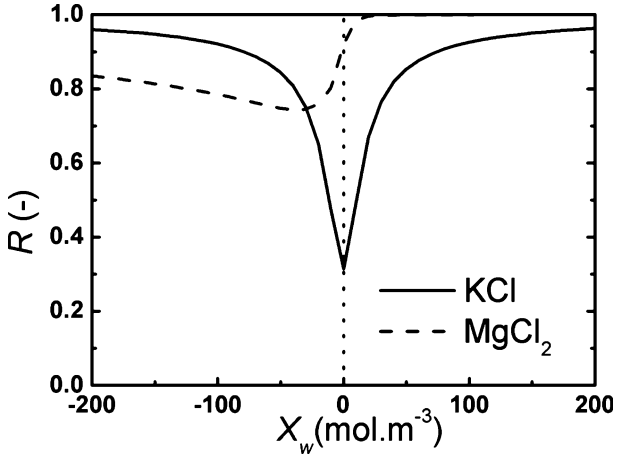

Fig. 9. Rejection as function of effective volume charge density X_w. $c_f = 10$ mol m^{-3}; $J_v = 12 \times 10^{-6}$ m^3 m^{-2} s^{-1}; $\Delta x/A_k = 10^{-4}$ m; $r_p = 0.4$ nm.

3.5. Effect of effective volume charge density on potentials

It is shown that potentials and rejection as a function of X_w for KCl and $MgCl_2$ at 10 mol m^{-3} in Figs. 8 and 9. For KCl, potentials and rejection show symmetry. The same diffusion coefficient of K^+ and Cl^- leads to zero values of potentials and minimum of rejection in neutral membranes. Zero values of potentials and minimum of rejection for $MgCl_2$ locate on that X_w is negative. The diffusion coefficient of Mg^{2+} is smaller than Cl^-, membrane potential will not equal to zero if concentration difference exists between both sides of membranes. And also if steric-hindrance effect cannot be ignored, Mg^{2+} with large steric coefficient will run slower than Cl^-, and convection potential is negative in neutral membranes. As mentioned in Ssection 3.2, when $t_{1m}/z_1+t_{2m}/z_2 = 0$ (that is $-z_1c_{1m}/z_2c_{2m}=D_{2p}/D_{1p}$), membrane potential equals to zero. By the same simplification, zero point of convection potential also can be obtained when $-z_1c_{1m}/z_2c_{2m} = K_{2c}/K_{1c}$. If there is no steric-hindrance effect, which means $D_{ip} = D_i$ and $K_{ic} = 1$, convection potential is zero in neutral membranes, and so is membrane potential for there will be no rejection. Under this situation, isoelectric point of membranes is the same in all kinds of solutes by judging from zero value of TMEP. But if steric-hindrance effect exists, and if $D_1 < D_2$ (that is, $r_{s1}>r_{s2}$, $K_{1c}<K_{2c}$), zero points of three potentials will locate on that X_w is negative. Moreover, X_w is more negative when D_1 is far from D_2. Oppositely, if $D_1>D_2$ (that is, $r_{s1}<r_{s2}$, $K_{1c}>K_{2c}$), zero points will appear when X_w is positive, and as D_2/D_1 is far from unit, X_w is more positive.

Szymczyk [22] did experiments on systems of plate ceramic membranes and three different solutions, and got isoelectric point of membranes by streaming

potential. Isoelectric points obtained in the solution of $CaCl_2$ are largest and the ones obtained in the solution of Na_2SO_4 are smallest. Besides the difference of ions absorption on membranes, the different diffusion coefficient of ions may be another factor that causes the excursion of isoelectric points. Because $D(Ca^{2+})<D(SO_4^{2-})<D(Na^+)<D(Cl^-)$, potentials in $CaCl_2$ should be zero when X_w is most negative, and in Na_2SO_4□X_w should be positive. This rule is completely confirmed by the experimental results. It is suggested that when TMEP is measured in different pH to judge the isoelectric point, the experiments had better been carried out in a solution with the solute which $D_1=D_2$ such as KCl.

And reflection coefficient will get lowest when membrane potential is zero as mentioned above. And if $D_1<D_2$, the inflexion of reflection coefficient locates on that X_w is negative. If $D_1>D_2$, the situation is opposite. Labbez [23]investigated rejection of five salts in different pH, and its results showed great agreement with our discussion.

4. Conclusions

A theoretical analysis of the effect of solution characters, membrane structures and electrical charge parameters on potentials (TMEP, including convection potential and membrane potential) arising in NF process was studied based on electrostatic and steric-hindrance model.

On the basis of the study of different electrolyte solutions (electrovalence, concentration and diffusion coefficients ratio of co-ion over counterion), the following conclusions can be made. With the existence of membrane potential, the dependencies of TMEP on solution flux are nonlinear. An increase of concentration leads to decrease of potentials, and membrane potential will become negative when concentration is large enough in $MgCl_2$. Concentration which leads to zero value of membrane potential coincides with that leads to minimum of reflection coefficient. When ξ_f^{-1} was larger than 50 in KCl solution and 100 in $MgCl_2$ solution, the electrostatic effect could almost be neglected, and potentials and reflection coefficient tend to be constant. As diffusion coefficient of counterions decrease, curves of potential behave distinctly in different concentration ranges. When ξ_f^{-1} is larger than 50 for 1-1 electrolytes, and for 2-1 electrolytes when ξ_f^{-1} is larger than 100, TMEP, membrane potential and convection potential will cross at $D_2/D_1=1.0$ for the neglectable electrostatic effect.

The effects of membranes structures and electrical charge parameters were also investigated. Without concerning steric-hindrance effect caused by small pore, potentials will be underestimated. $\Delta x/A_k$ has more influence on convection potential. When it is large enough, it is proportional to convection potential and does nothing with membrane potential. Potentials in KCl solution show symmetry as effective volume charge density changes from positive to negative for diffusion coefficient of K^+ is almost the same as Cl^-. Zero points of potentials in $MgCl_2$ solution locate on that effective volume charge density is negative. It is suggested that when TMEP is measured in different pH to judge isoelectric point of NF membranes with small pores, solutes with $D_1\neq D_2$ are not advised to use in order to avoid overestimation or underestimation.

ES model is suitable to analyze the potentials arising in NF process with the pressure drop and concentration difference. The results give a comprehensive vision on changes of potentials under different circumstance. TMEP across NF membranes should be advised to be analyzed carefully by combining the convection potential and membrane potential. Experiments would be carried out to testify the theoretical results later on.

Nomenclature

A_k	membrane Porosity (–)
c	concentration (mol m^{-3})
D_i	diffusion coefficient of ions I (m^2 s^{-1})
D_{ip}	effective diffusion coefficient of ions i (m^2 s^{-1})
F	Faraday constant (=96,487) (C mol^{-1})
H_{Di}	steric-hindrance parameters related to the wall correction factors of ions i under diffusion condition (–)
H_{Fi}	steric-hindrance parameters related to the wall correction factors of ions i under convection condition (–)
I	current density (A m^{-2})
i_c	convection current density (A m^{-2})
i_{cm}	averaged convection current density in membranes (A m^{-2})
J_v	solution volume flux over the membrane surface (m^3 m^{-2} s^{-1})
J_i	ion flux over the membrane surface (mol m^{-2} s^{-1})
J_v	solution volume flux over the capillary cross-section (m^3 m^{-2} s^{-1})
J_i	ion flux over the capillary cross-section (mol m^{-2} s^{-1})
k_i	local distribution coefficient of ion (–)
K_{ic}	convection hindrance factor of ions i (–)
K_{id}	diffusion hindrance factor of ions i (–)
L_p	pure water permeability of capillary (m^3 m^{-2} s^{-1} Pa^{-1})
r_{si}	Stokes radius of ions i (m)

r_p membrane pore radius (m)
R rejection (–)
R_g gas constant (8.314) (J mol^{-1} K^{-1})
S_{Di} contribution to the averaged distribution coefficients caused by the steric-hindrance effects of ions under diffusion condition (–)
S_{Fi} contribution to the averaged distribution coefficients caused by the steric-hindrance effects of ions under convection condition (–)
t_i transport number of ions i (–)
t_{im} averaged transport number of ions i in membranes (–)
T temperature (K)
T_r transmission rate (–)
x axial variable of capillary (m)
Δx the effective membrane thickness (m)
X_w effective volume charge density (mol m^{-3})
z_i electrochemical valence of ion (–)

Greek letter

$\Delta\varphi$ electric potential (V)
$\Delta\varphi_c$ convection potential (V)
$\Delta\varphi_d$ diffusion potential (V)
$\Delta\varphi_D$ Donnan potential (V)
$\Delta\varphi_m$ membrane potential (V)
$\Delta\varphi_T$ TMEP (V)
η_i ratio of Stokes radius of ions to pore radius (–)
κ electric conductance (S m^{-1})
κ_m averaged electric conductance in membranes (S m$^{-1)}$
ξ equals to X_w/z_1v_1c (–)
θ equals to $\exp(-F\Delta\varphi_D/R_gT)$ (–)
σ reflection coefficient (–)
ω solute permeability coefficient (mol m^2 J^{-1} s^{-1})

Subscripts

i ith ion (=1 —counterion; =2 —co-ion)
m membrane phase
f feed side
p permeate side

References

[1] J. Benavente and G. Jonsson, Electrokinetic characterization of composite membranes: estimation of different electrical contributions in pressure induced potential measured across reverse osmosis membranes, J. Membr. Sci., 172 (1–2) (2000) 189–197.
[2] J. Benavente and G. Jonsson, Influence of the external conditions on salt retention and pressure-induced electrical potential measured across a composite membrane, Coll. Surf. A–Physicochem. Eng. Asp., 159 (2–3) (1999) 431–437.
[3] A. Szymczyk, M. Sbai, and P. Fievet, Analysis of the pressure-induced potential arising through composite membranes with selective surface layers, Langmuir, 21 (5) (2005) 1818–1826.
[4] P. Fievet, M. Sbai and A. Szymczyk, Analysis of the pressure-induced potential arising across selective multilayer membranes, J. Membr. Sci., 264 (1–2) (2005) 1–12.
[5] A.E. Yaroshchuk, Y.P. Boiko and A.L. Makovetskiy, Filtration potential across membranes containing selective layers, Langmuir, 18 (13) (2002) 5154–5162.
[6] M. Elimelech,W.H. Chen and J.J. Waypa, Measurin the zeta (electrokinetic) potential of reverse-osmosis membranes by a streamin potential analyzer, Desalination, 95 (3) (1994) 269–286.
[7] M. Mullet, P. Fievet, A. Szymczyk et al., A simple and accurate determination of the point of zero charge of ceramic membranes, Desalination, 121 (1) (1999) 41–48.
[8] W.J. Shang, X.L. Wang, and H.L. Wang, Modeling on electrokinetic phenomena of charged porous membrane, Desalination, 233 (1–3) (2008) 342–350.
[9] P. Fievet, B. Aoubiza, A. Szymczyk et al., Membrane potential in charged porous membranes, J. Membr. Sci., 160 (2) (1999) 267–275.
[10] C. Lettmann, D. Mockel and E. Staude, Permeation and tangential flow streaming potential measurements for electrokinetic characterization of track-etched microfiltration membranes, J. Membr. Sci., 159 (1–2) (1999) 243–251.
[11] X. Lefebvre, J. Palmeri and P. David, Nanofiltration theory: An analytic approach for single salts, J. Phys. Chem. B, 108 (43) (2004) 16811–16824.
[12] X. Lefebvre and J. Palmeri, Nanofiltration theory: Good co-ion exclusion approximation for single salts, J. Phys. Chem. B, 109 (12) (2005) 5525–5540.
[13] X.L. Wang, T. Tsuru, M. Togoh et al., Transport of organic electrolytes with electrostatic and steric-hindrance effects through nanofiltration membranes, J. Chem. Eng. Jap., 28(4) (1995) 372–380.
[14] X.L. Wang, T. Tsuru, S. Nakao et al., The electrostatic and steric-hindrance model for the transport of charged solutes through nanofiltration membranes, J. Membr. Sci., 135 (1) (1997) 19–32.
[15] S. Nakao and S. Kirnura, Models of membrane transport phenomena and their appplications for ultrafiltration data, J. Chem. Eng. Jap., 15 (1982) 200–205.
[16] A. Szymczyk and P. Fievet, Investigating transport properties of nanofiltration membranes by means of a steric, electric and dielectric exclusion model, J. Membr. Sci., 252 (1–2) (2005) 77–88.
[17] A.E. Yaroshchuk, Dielectric exclusion of ions from membranes, Adv. Coll. Interf. Sci., 85 (2–3) (2000) 193–230.
[18] W.J. Shang, X.L. Wang and Y.X. Yu, Theoretical calculation on the membrane potential of charged porous membranes in 1-1, 1-2, 2-1 and 2-2 electrolyte solutions, J. Membr. Sci., 285 (1–2) (2006) 362–375.
[19] H.J.M. Hijnen, J. Vandaalen and J.A.M. Smit, The application of the space-charge model to the permeability properties of charged microporous membranes, J. Coll.Interf. Sci., 107 (2) (1985) 525–539.
[20] C.H. Tu, H.L. Wang and X.L. Wang, Study on transmembrane electrical potential of nanofiltration membranes in KCl and MgCl2 solutions, Langmuir, 26 (22) (2010) 17656–17664.
[21] X.L. Wang, T. Tsuru, S. Nakao et al.,Electrolyte transport through nanofiltration membranes by the space-charge model and the comparison with Teorell-Meyer-Sievers model, J. Membr. Sci., 103 (1–2) (1995) 117–133.
[22] A. Szymczyk, P. Fievet, M. Mullet et al., Comparison of two electrokinetic methods – electroosmosis and streaming potential – to determine the zeta-potential of plane ceramic membranes, J. Membr. Sci., 143 (1–2) (1998) 189–195.
[23] C. Labbez, P. Fievet, A. Szymczyk et al., Analysis of the salt retention of a titania membrane using the ''DSPM'' model: effect of pH, salt concentration and nature, J. Membr. Sci., 208(1–2) (2002):315–329.